International Journal of Chemistry Studies
ISSN: 2581-348X; Impact Factor: RJIF 5.44
Received: 19-03-2019; Accepted: 24-04-2019
www.chemistryjournal.in
Volume 3; Issue 3; May 2019; Page No. 46-52

Spectroscopy analysis and molecular docking of toxic interaction mechanism of tartrazine with Pepsin

Hongcai Zhang[1], Baosheng Liu[2*], Xu Cheng[3]
[1, 2, 3] College of Chemistry & Environmental Science, Hebei University, Baoding, Hebei, China

Abstract
The interaction between tartrazine (TTZ) and pepsin (PEP) was studied by various spectroscopy and molecular docking simulation techniques under the experimental conditions of pH=2.20. The results showed that TTZ could effectively quench the endogenous fluorescence of PEP, formed a 1:1 complex. The thermodynamic parameters were obtained from the van't Hoff equation, and the Gibbs free energy $\Delta G<0$, indicating that the reaction was spontaneous; $\Delta H<0$, $\Delta S>0$, indicating hydrophobic interaction played a major role in forming the TTZ-PEP complex. Molecular docking results showed that TTZ was bound in the hydrophobic cavity of PEP and surrounded by active amino acid residues Asp32 and Asp215, which changed the microenvironment of amino acid residues at the catalytic active center of PEP. Furthermore, as shown by the synchronous fluorescence, UV-Vis absorption and circular dichroism data, TTZ could lead to the conformational changes of PEP, which might affect its physiological function.

Keywords: tartrazine, pepsin, spectroscopy, molecular docking, interaction

1. Introduction
PEP is a digestive protease which is released by the main cells in the stomach [1]. PEP, molecular weight of 35,000 Da, has a single polypeptide chain with 327 amino acid residues [2]. The catalytic site is formed by two aspartic acid residues Asp32 and Asp215, one of which must be protonated and the other deprotonated to make the protein active [3]. Lack of PEP, the body's protein metabolism ability will be severely inhibited, resulting in gastrointestinal discomfort and even severe digestive diseases.TTZ (the structural formula is shown in Fig. 1) is a synthetic acid azo dye with an aqueous solution in yellow. As a coloring agent, it is widely used in sugar coatings and capsules for cakes, confectionery, beverages and pharmaceutical preparations [4]. Some reports also point out that TTZ can cause allergic reactions, hyperactivity, irritability and sleep disorders in children [5]. In general, synthetic dyes usually contain azo functional groups and aromatic ring structures, which are harmful to human health. Long-term intake of foods containing large amounts of TTZ can cause allergies, migraine, eczema, anxiety, and the impact on the digestive system is also very obvious, such as nausea, vomiting, abdominal pain, diarrhea, *et al*. [6].
In recent years, fluorescence spectroscopy has become an important means to study the mechanism of action of ligand-protein systems. So far, Liu Zhidong and his companions found that TTZ could quench the fluorescence of bovine serum albumin by static quenching [7]. Anirban Basu and his companions used various spectroscopy methods to explore the mechanism of action of TTZ and human hemoglobin [8]. As an important digestive protease in the human body, PEP is inevitably in contact with food, which may affect the structure and properties of PEP. Therefore, the interaction between TTZ and PEP was studied by using multiple spectroscopy methods and molecular docking techniques. The results may be helpful to complement the limited toxicity literature for TTZ, and will also provide a new approach to probe the toxicity of TTZ at the molecular level.

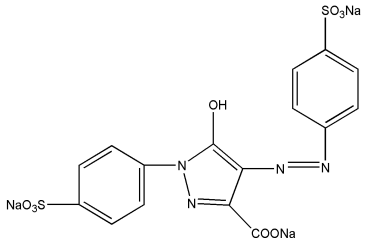

Fig 1: Chemical structure of TTZ

2. Materials and Methods
2.1 Apparatus
These fluorescence spectra were acquired with a Shimadzu RF-5301PC spectrofluorophotometer. Circular dichroism spectra were recorded on a MOS-450/SFM300 circular dichroism spectrometer (Bio-Logic, France). Absorption was measured with an UV-vis recording spectrophotometer (UV-3600, Shimadzu, Japan). All pH measurements were made with a pHS-3C precision acidity meter (Leici, Shanghai, China). All temperatures were controlled by a SYC-15$_B$ superheated water bath (Sangli, Nanjing, China).

2.2 Materials
PEP was purchased from Sigma-Aldrich (purity grade inferior 99%, Shanghai, China), standard solution (5.0×10^{-5} mol/L) was prepared. TTZ standard solution (1.0×10^{-3} mol/L) was prepared. Citric acid-disodium phosphate buffer solution was used to keep the pH of the solution at 2.20, and NaCl (0.10 mol/L) solution was used to maintain the ionic strength of the solution. All other reagents were analytical grade and all aqueous solutions were prepared with newly double-distilled water and stored at 277 K.

The fluorescence intensity measured in the experiment was corrected by the "internal filter effect" Eq.(1) [9]:

$$Icor = Iobs \times e^{(A_{ex}+A_{em})/2} \quad (1)$$

Where I_{cor} and I_{obs} are the fluorescence intensities corrected and observed, respectively, and A_{ex} and A_{em} are the absorption of the system at the excitation and the emission wavelength, respectively. The intensity of fluorescence used in this paper is the corrected fluorescence intensity.

2.3 Methods

2.3.1 Fluorescence measurements

1.0 mL Citric acid-disodium phosphate buffer solution (pH=2.20), 2.0 mL PEP (1.0×10^{-5} mol/L), and different volumes of TTZ were added into 10 mL colorimetric tube successively. The samples were diluted to scaled volume with double-distilled water, mixed thoroughly by shaking, and kept static for 30 min at different temperatures (298 K, 310 K, and 318 K). Excitation wavelength with excitation and emission slit at 5 nm for PEP as 280 and 295 nm, respectively. The solution was subsequently scanned on the fluorophotometer and determined the fluorescent intensity. At the same time fixed $\Delta\lambda$=15 nm or $\Delta\lambda$=60 nm, the synchronous fluorescence spectra of TTZ and PEP were recorded.

2.3.2 UV-vis measurements

1.0 mL Citric acid-disodium phosphate buffer solution (pH=2.20), 2.0 mL PEP solution (1.0×10^{-5} mol/L) and different volumes of TTZ were successively added to a 10 mL colorimetric tube, and the reference solutions were the corresponding concentration of TTZ solutions. The samples were diluted to scaled volume with water, mixed thoroughly by shaking, and kept static for 30 min at 298 K. The UV-vis absorption spectrum of TTZ in the presence and absence of PEP were scanned with 1cm quartz cells over the range from 190 nm to 400 nm.

2.3.3 Circular dichroism measurements

A total of 1.0 mL Citric acid-disodium phosphate buffer solution (pH=2.20), 2.0 mL PEP solution (1.0×10^{-5} mol/L), and different volumes of TTZ were added into a 10 mL colorimetric tube successively. The samples were diluted to scaled volume with water, mixed thoroughly by shaking, and kept static for 30 min at 298 K. Circular dichroism measurements were performed with a 1.0 cm path length quartz cuvette. Each spectrum was recorded at wavelengths between 190 and 300 nm and a scan speed of 1 nm/s.

2.3.4 Molecular docking

The two-dimensional structure of TTZ was drawn in ChemDraw 15.0, and its three-dimensional structure was optimized by model of molecular mechanics in ChemDraw 3D. The crystal structure of PEP used for molecular docking was obtained from protein data bank (PDB ID: 5PEP). Waters and all other HETATM molecules were removed from the PDB file of PEP. Polar hydrogen atoms and Gasteiger charges were added to prepare the PEP molecule for docking. Protein-ligand docking was performed with the rigid docking tool in the Autodock 4.2.6. In this work, the selection of flexible residues for the induced fit is based on the active site of the PEP. The most favorable docking model was selected according to the binding energy and the geometry matching [10].

3. Results and Discussion

3.1 The Fluorescence spectra of TTZ-PEP system

At 280nm wavelength, the Trp and Tyr residues in PEP are excited, whereas a wavelength of 295nm excites only Trp residues [11]. Fig. 2 showed that the fluorescence emission spectrum of PEP when TTZ was added at different concentrations. A typical emission peak was observed at about 348 nm when the excitation wavelength is λ_{ex}=280 nm. (The fluorescence emission spectrum of TTZ-PEP was similar to λ_{ex}=295 nm, but the fluorescence intensity is low.) As the TTZ concentration increased, the degree of fluorescence quenching increased, and the maximum emission peak was blue-shifted, indicating that TTZ interacted with PEP and formed a stable complex [12].

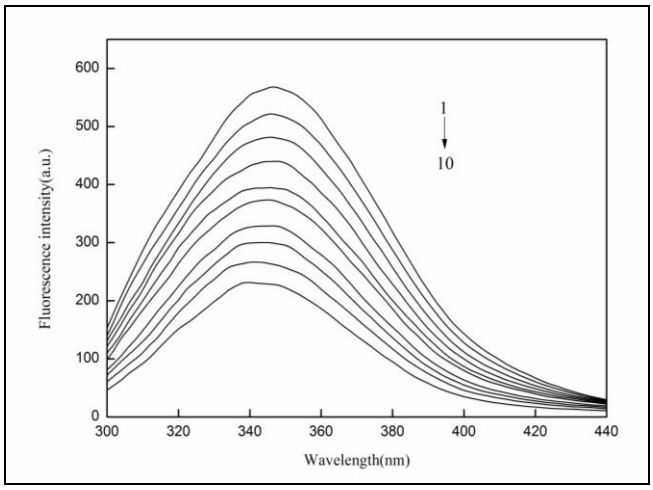

Fig 2: Fluorescence emission spectra of TTZ-PEP system (T=298 K, λ_{ex}=280 nm) $C_{PEP}=2.0\times10^{-6}$ mol/L, 1~10 C_{TTZ}=(0, 0.5, 1.0, 1.5, 2.0, 3.0, 4.0, 5.0, 6.0, 7.0)$\times10^{-5}$ mol/L

In order to study the quenching mechanism, the quenching data was processed according to the Stern-Volmer Eq. (2) [13], and the results were shown in Table 1.

$$I_0/I = 1 + k_q\tau_0[L] = 1 + K_{sv}[L] = 1 + KD[L] \quad (2)$$

Where, I_0 and I are the fluorescence intensities of PEP in the absence and presence of the TTZ, respectively. K_q is the bimolecular quenching constant and [L] is the concentration of the quencher, τ_0 is the average lifetime of fluorescence (about 10^{-8} s) and K_{sv} is the Stern-Volmer quenching constant. From Table 1, it could be seen that the K_q value was greater than 2.0×10^{10} L/mol·s at different temperatures [14]. The K_{sv} value was inversely correlated with temperatures. The result indicated that the combination process of TTZ-PEP system was a static quenching process.

Table 1: Quenching reactive parameters of TTZ-PEP system at different temperature

λ_{ex} (nm)	T (K)	K_{sv} (L/mol·s)	K_q (L/mol)	r_1	K_a (L/mol)	n	r_2
λ_{ex}=280	298	4.07×10^4	4.07×10^{12}	0.9928	3.82×10^4	1.08	0.9948
	310	3.75×10^4	3.75×10^{12}	0.9978	3.40×10^4	1.06	0.9923
	318	3.11×10^4	3.11×10^{12}	0.9965	2.95×10^4	1.22	0.9915
λ_{ex}=295	298	3.22×10^4	3.22×10^{12}	0.9912	2.99×10^4	1.17	0.9919
	310	2.86×10^4	2.86×10^{12}	0.9936	2.62×10^4	1.12	0.9911
	318	2.47×10^4	2.47×10^{12}	0.9915	2.15×10^4	0.91	0.9962

r_1 is the linear relative coefficient of I_0/I~[L], r_2 is the linear relative coefficient of lg [(I_0-I)/I]~lg{[L]-n[B_t](I_0-I)/I_0}.

The relationship between fluorescence intensity and the concentration of quencher can usually be described using Eq. (3) [15] to obtain the binding constant (K_a) and the number of binging sites (n):

$$lg\left(\frac{I_0-I}{I}\right) = n\,lg\,K_a + n\,lg\left\{[L] - n\frac{I_0-I}{I0}[B_t]\right\} \quad (3)$$

Where [L] and [B_t] are the concentrations of TTZ and PEP, respectively. On the assumption that n in the bracket is equal to 1, the curve of lg(I_0-I)/I versus lg{[L]-n[B_t](I_0-I)/I} is drawn and linearly fitted, then the value of n can be obtained from the slope of the plot. On the basis of value of n obtained, the binding constant K_a can also be determined. The results were listed in the Table 1.The results showed that all the values of n were approximately equal to 1 at different temperatures, indicating that TTZ had only one high-affinity binding site when bound to PEP [16]. When the temperature rose, the binding constant K_a value showed a decreasing trend, and the binding ability of TTZ to PEP was reduced, which further proved that the TTZ-PEP system was static quenching. Fig.3 showed the involvement of Tyr and Trp residues in PEP. As can be seen in Fig. 3, the fluorescence quenching curve at λ_{ex}=280 and 295 nm was separated, and the fluorescence quenching curve of λ_{ex}=280 nm is lower than that at λ_{ex}=295 nm, implying that both Trp and Tyr residues of PEP participated the reaction and the Trp residues involvement was larger than that of Tyr residues.

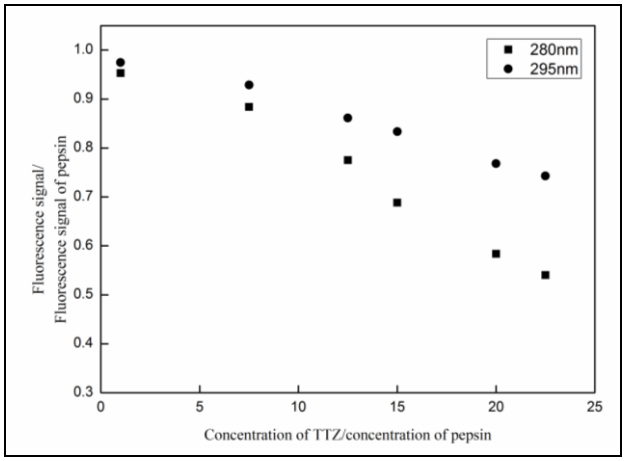

Fig 3: Fluorescence emission spectra of TTZ-PEP at λ_{ex}=280 nm and 295 nm (T=298 K) C_{PEP}=2.0×10^{-6} mol/L, C_{TTZ}= (0.5, 1.5, 2.5, 3.0, 4.0, 4.5) $\times10^{-5}$ mol/L

3.2 Type of interaction force of TTZ-PEP system

The signs and magnitudes of the thermodynamic parameters (ΔH, ΔS and ΔG) in the binding process of biomacromolecule with small molecule can be used to confirm the binding modes. These thermodynamic parameters can be calculated by the van't Hoff equations [17].

$$R\,ln\,K = \Delta S - \Delta H/T \quad (4)$$

$$\Delta G = \Delta H - T\Delta S \quad (5)$$

Table 2: The thermodynamic parameters of TTZ-PEP at different temperatures

system	T/(K)	K_a/(L/mol)	ΔH/(kJ/mol)	ΔS/(J/mol·K)	ΔG/(kJ/mol)
λ_{ex}= 280 nm	298	3.82×10^4	-16.52	29.74	-25.39
	310	3.40×10^4		30.54	-25.99
	318	2.95×10^4		29.61	-25.94

Where ΔH and ΔS represent the standard variation of the enthalpy and, respectively, entropy of the binding process. R is the gas constant (R=8.314 J/mol·K), T is the absolute temperature. Based on the linear fit plot of $R\ln K_a$ versus 1/T, the ΔH and ΔS values can be obtained. The results obtained are listed in Table 2. It can be seen from Table 2 that ΔG<0, indicating that the quenching reaction of TTZ to PEP was spontaneous; ΔS>0, suggesting that there was hydrophobic interaction between TTZ and PEP; ΔH<0 cannot be used as a sign of inter molecular electrostatic attraction, Ross pointed out that when $\Delta H\approx0$, ΔS>0, it could be considered as electrostatic attraction, and ΔH<0 is considered as the result of hydrogen bonding [18-20]. Therefore, the force between TTZ and PEP was mainly hydrophobic interaction and hydrogen bonding.

In general, electrostatic force plays a supporting role in the binding of proteins and ligands. However, if electrostatic interactions plays a dominant role in the binding of proteins to small molecules, the interaction intensity decreases as the salt concentration increases in the system [21]. In order to further verify the existence of electrostatic interaction between TTZ and PEP, the effect of ionic strength on TTZ-PEP interaction was discussed.

The concentrations of TTZ and PEP were fixed, and different concentrations of NaCl were added, and I/I_0 was plotted against C_{NaCl}. The results were shown in Fig. 4. The experimental results showed that the ratio of I/I_0 did not change significantly when the concentration of NaCl increased, indicating that the combination of TTZ and PEP was not affected by ionic strength, that is, the TTZ-PEP system had no obvious electrostatic effect. This conclusion was the same as the conclusion of the thermodynamic constant.

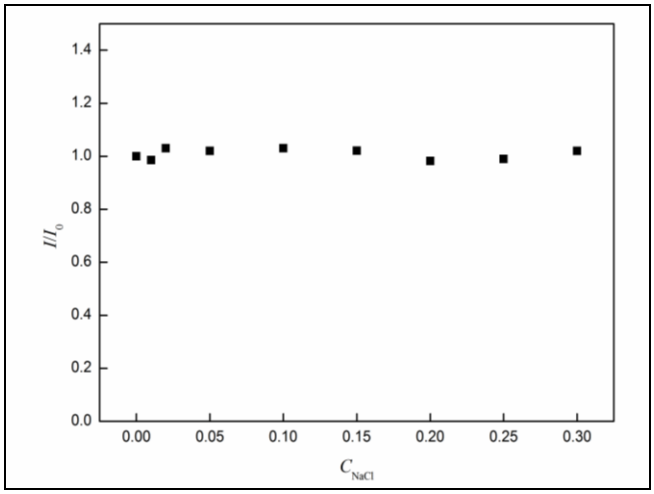

Fig 4: Fluorescence intensity of TTZ-PEP system as a function of NaCl concentration (T=298 K) C_{PEP} =2.0×10^{-6} mol/L, C_{TTZ}= 1.0×10^{-5} M, C_{Nacl} = (0, 0.1, 0.2, 0.5, 1.0, 1.5, 2.0, 2.5, 3.0) ×10^{-1} mol/L

3.3 Investigation of PEP conformation changes

3.3.1 Synchronous fluorescence studies of TTZ-PEP system

For synchronous fluorescence spectra of proteins, when the $\Delta\lambda$ value between the excitation and emission wavelengths is stabilized at 15 or 60 nm, the synchronous fluorescence gives characteristic information for Tyr or Trp residues [22]. Fig.5 (A and B) showed the effects of TTZ on the synchronous fluorescence spectra of PEP. It can be seen from Fig. 5 that when $\Delta\lambda$=15 nm or $\Delta\lambda$=60 nm, the fluorescence intensity of PEP decreased with the increase of TTZ concentration, showing that Tyr and Trp residues both participated in the interaction of TTZ with PEP. In addition, the maximum emission wavelength of Tyr and Trp residues had a slightly red shift, suggesting that the microenvironment of these residues became more hydrophobic and polarity enhancement. The results indicated that the TTZ caused a change in the conformation of the PEP.

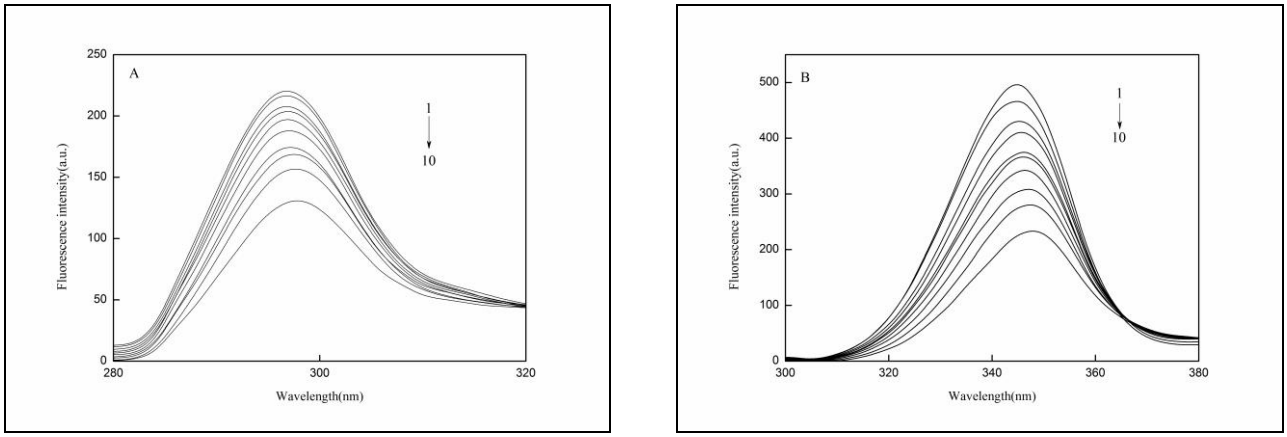

Fig 5: Synchronous fluorescence spectra of TTZ-PEP system (T=298 K). (A) $\Delta\lambda$=15 nm; (B) $\Delta\lambda$=60nm C_{PEP}=2.0×10^{-6} mol/L, 1~10 C_{TTZ}=(0, 0.5, 1.0, 1.5, 2.0, 3.0, 4.0, 5.0, 6.0, 7.0)×10^{-5} mol/L

3.3.2 UV-vis absorption spectra studies of TTZ-PEP system

The UV-vis absorption spectra of TTZ-PEP system was shown in Fig. 6. PEP had two absorption peaks, the strong absorption peak at about 208 nm reflects the framework conformation of the protein, the weak absorption peak at about 280 nm appears to be due to the aromatic amino acids (Trp, Tyr, and Phe) [23]. With gradual addition of TTZ to PEP solution, the intensity peak of pepsin at 208 nm decreased with a red shift and the intensity of the peak at 280 nm had minimal changes (Fig. 6). The intensity of the absorption peak at 280 nm was reduced, illustrating that the interaction between TTZ and PEP happened in the ground-state molecules. That is to say, non-luminous complex formed in ground state of TTZ and PEP, which led to the change of UV-vis absorption spectra of PEP. Dynamic quenching only affects the excited states of fluorescent molecule, and does not alter the absorption spectra of the fluorescent substance. The results showed that type of fluorescence quenching of TTZ-PEP system was static quenching [24]. This conclusion was consistent with the conclusion of the fluorescence quenching experiment.

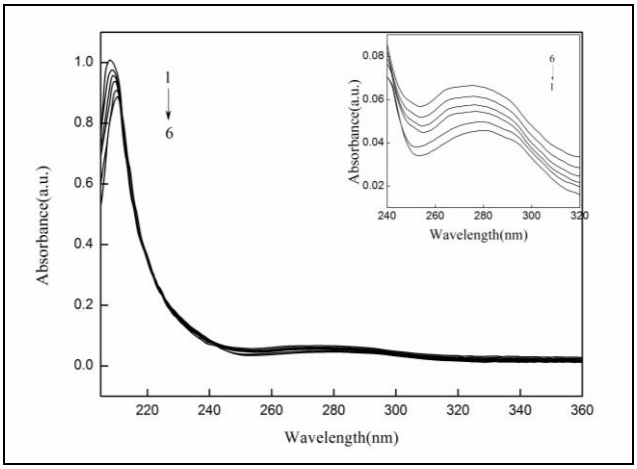

Fig 6: Absorption spectrum of TTZ-PEP system (T=298 K) C_{PEP}=2.0×10^{-6} mol/L, 1~6: C_{TTZ}=(0, 1.0, 2.0, 3.0, 4.0, 5.0)×10^{-5} mol/L

3.3.3 Circular dichroism spectra studies of TTZ-PEP system

Circular dichroism spectroscopy (CD) is commonly used to

detect changes in the secondary structure of proteins. The CD spectrum of the TTZ-PEP system was shown in Fig. 7. It can be seen from Fig. 7 that the characteristic peak at 208 nm is the characteristic peak of the α-helix structure in PEP [25]. When the concentration ratio of PEP to TTZ was 1:0, 1:5 and 1:10, the α-helix content of PEP decreased from 33.10% to 23.10%. As the concentration of TTZ increased, the absorption intensity of the negative peak gradually decreased, implying that TTZ caused a change in the secondary structure of PEP, and made the protein structure loose. But the peak shape and peak position had not been changed, indicating that the α-helix in the PEP molecule still dominated.

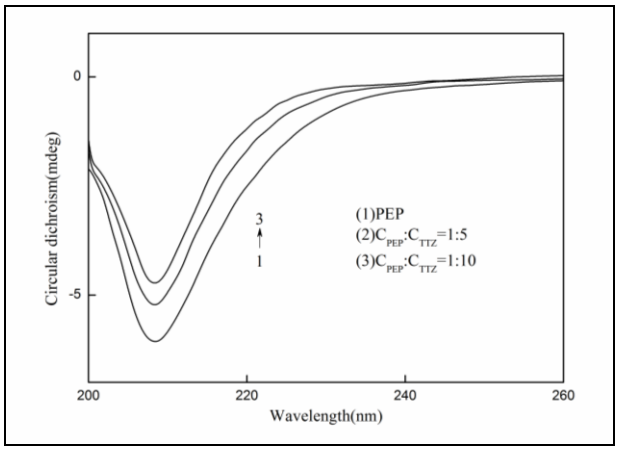

Fig 7: The circular dichroism spectra of TTZ-PEP system (T=298 K) C_{PEP} = 2.0×10^{-6} mol/L; C_{TTZ} = (0, 1.0, 2.0)×10^{-5} mol/L.

3.5 Molecular docking

Molecular docking method can simulate the interaction between small molecules and proteins at the atomic level, so that it can find small molecules at the target protein binding site and clarify interesting biochemical processes. The best combination mode predicted by the docking software Autodock 4.2.6 was shown in Fig. 8.

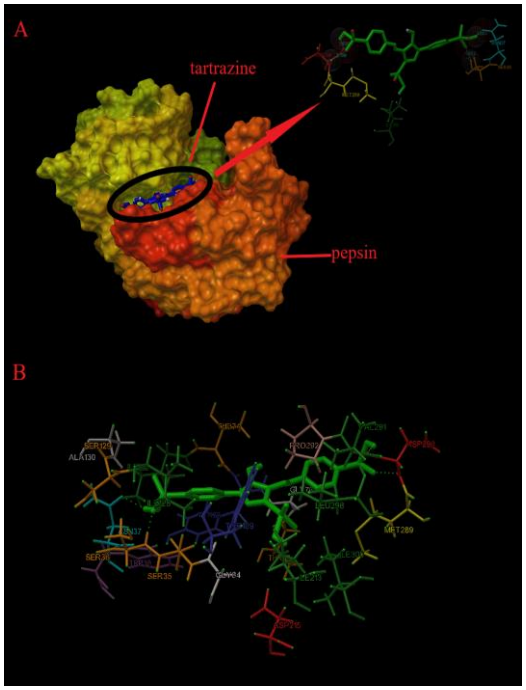

Fig 8: Computation docking model of the interaction between TTZ and PEP

TTZ located within the hydrophobic pocket in PEP (B) Detailed illustration of the amino acid residues lining the binding site in the TTZ and PEP cavity

Figure 8(A) showed the best binding position between TTZ and PEP. Asn37 and Ser36 formed two hydrogen bonds with TTZ, respectively. The bond lengths were 2.083 Å and 1.683 Å, respectively. Asn290 formed two hydrogen bonds with TTZ and the bond lengths were 2.199 Å and 1.396 Å, respectively, indicating that hydrogen bonding played a very important role in the combination of TTZ and PEP. At the same time, the low free energy binding site of TTZ on PEP was also given. TTZ was bound in the hydrophobic cavity of PEP and surrounded by active amino acid residues Asp32 and Asp215, which changed the microenvironment of amino acid residues at the catalytic active center of PEP. Figure 8(B) showed the presence of multiple hydrophobic amino acid residues around TTZ such as Ala130, Ile128, Trp39, Tyr75, Tyr189, Pro292, Val291, Met289, Leu298, indicating the presence of hydrophobic interactions during the binding of TTZ and PEP. In the docking process, the minimum free energy binding energy of TTZ-PEP complex was -24.64 kJ/mol, which was close to the experimental data (-25.39 kJ/mol). This difference might be due to exclusion of the solvent in docking simulations or rigidity of the receptor other than Trp and Tyr residues [26]. The energy data obtained by docking the molecules are listed in Table 4. From Table 4, it could be also seen that the electrostatic energy was very much lower than the sum of Vander Waals energy, hydrogen bonding energy and desolvation free energy in the binding process of TTZ with PEP, implying that the main interaction mode between TTZ and PEP was not electrostatic binding mode. This was also consistent with the effect of ionic strength on the fluorescence experiment of TTZ-PEP binding. The binding position of PEP was near to that of Trp39, Tyr75 and Tyr189, suggesting that both Tyr and Trp residues participated in the reaction, which was consistent with the fluorescence quenching experiment. Through fluorescence experiments and molecular docking, it could be inferred that TTZ and PEP were combined by hydrophobic force and hydrogen bonding, resulting in static quenching of PEP fluorescence.

Table 3: Docking energy of TTZ-PEP system (unit: kJ/mol)

Protein PDB ID	ΔG_0	ΔE_1	ΔE_2	ΔE_3
5PEP	-24.64	-25.81	-23.59	-1.05

ΔG_0 is the binding energy in the binding process.
ΔE_1 denotes intermolecular interaction energy, which is a sum of van der Waals energy, hydrogen bonding energy, desolvation free energy and electrostatic energy.
ΔE_2 is the sum of van der Waals energy, hydrogen bonding energy and desolvation free energy.
ΔE_3 is the electrostatic energy.

4. Conclusion

In this paper, the interaction mechanism between TTZ and PEP was studied by using multiple spectroscopy methods and molecular docking simulation techniques under simulated physiological conditions. During the fluorescence spectroscopic and computational analysis, TTZ quenched the fluorescence of PEP effectively to form a complex with only one site of protein mainly through hydrophobic force and hydrogen bond. The microenvironment and conformation of PEP were also changed by the bound TTZ as indicated by the UV-Vis absorption spectra, synchronous

fluorescence spectra and CD spectra. Experiments have proved that TTZ has a strong binding ability to PEP, which provides theoretical guidance for further understanding the toxicity of colorants to human and further studies are needed to provide for health risk assessment of food colorants.

5. Acknowledgments

The authors gratefully acknowledge the financial support of National Science Foundation of China (Grant no. 21375032).

6. References

1. Shen LL, Xu H, Huang FW, Li Y, Xiao HF, Yang Z, *et al.* Investigation on interaction between Ligupurpuroside A and pepsin by spectroscopic and docking methods. Spectrochim Acta A Mol Biomol Spectrosc. 2015; 135(7):256-263.
2. Wang YQ, Zhang HM. Comparative Studies of the Binding of Six Phthalate Plasticizers to Pepsin by Multispectroscopic Approach and Molecular Modeling. Journal of Agricultural and Food Chemistry. 2013; 61(46):11191-11200.
3. Zeng HJ, Liang HL, You J, Qu LB. Study on the binding of chlorogenic acid to pepsin by spectral and molecular docking. Luminescence, 2015; 29(7):715-721.
4. Mehedi N, Ainadtabet S, Mokrane N, Addou C, Zouai O, Kheroua O, *et al*. Reproductive toxicology of tartrazine (FD and C Yellow No. 5) in Swiss albino mice. American Journal of Pharmacology & Toxicology. 2009; 4(4):130-135.
5. McCann D, Barrett A, Cooper A, Crumpler D, Dalen L, Grimshaw K, *et al*. Food additives and hyperactive behaviour in 3-year-old and 8/9-year-old children in the community: a randomised, double-blinded, placebo-controlled trial. Lancet, 2007; 370(9598):1560-1567.
6. Dorraji PS, Jalali F. Electrochemical fabrication of a novel ZnO/cysteic acid nanocomposite modified electrode and its application to simultaneous determination of sunset yellow and tartrazine. Food Chemistry, 2017; 227:73-77.
7. Basu A, Kumar GS. Multispectroscopic and calorimetric studies on the binding of the food colorant tartrazine with human hemoglobin. Journal of Hazardous Materials. 2016; 318:468-476.
8. Liu ZD, Han DQ, Yang WW, Shao SS, Sun QS. Interactions of bovine serum albumin with lemon yellow and sunset yellow studied by fluorescence spectroscopy. Food Science, 2014; 35(9):128-131.
9. Ma LH, Liu BS, Wang CD, Zhang HC, Cheng X. The interaction mechanism of nifedipine and pepsin. Monatshefte für Chemie - Chemical Monthly, 2018; 149(11):2123-2130.
10. Elmas G, Esra Y. Fluorescence interaction and determination of sulfathiazole with trypsin. Journal of Fluorescence. 2014; 24(5):1439-1445.
11. Zhang LH, Liu BS, Li ZY, Guo Y. Comparative studies on the interaction of cefixime with bovine serum albumin by fluorescence quenching spectroscopy and synchronous fluorescence spectroscopy. Asian Journal of Chemistry. 2015; 30(5):686-692.
12. Mahaki H, Memarpoor-Yazdi M, Chamani J, Addou S, Zouai C. Interaction between ropinirole hydrochloride and aspirin with human serum albumin as binary and ternary systems by multi-spectroscopic, molecular modeling and zeta potential. Journal of Luminescence. 2013; 134(3):758-771.
13. Safarnejad A, Shaghaghi M, Dehghan G, Soltani S. Binding of carvedilol to serum albumins investigated by multi-spectroscopic and molecular modeling methods. Journal of Luminescence. 2016; 176:149-158.
14. Toprak M. Fluorescence study on the interaction of human serum albumin with butein in liposomes. Spectrochemica Acta Part A Molecular & Biomolecular Spectroscopy, 2016; 154:108-113.
15. Tian ZY, Zang FL, Luo W, Zhao ZH, Xu XY. Spectroscopic study on the interaction between mononaphthalimide spermidine (MINS) and bovine serum albumin (BSA). Journal of Photochemistry & Photobiology B Biology. 2015; 142(9):103-109.
16. Amroabadi MK, Taheri-kafrani A, Saremi LH, Rasteqai AA. Spectroscopic Studies of the interaction between alprazolam and apo-human serum transferrin as a drug carrier protein. International Journal of Biological Macromolecules. 2018; 108:263-271.
17. Naik KM, Nandibewoor ST. Spectroscopic studies on the interaction between chalcone and bovine serum albumin. Journal of Luminescence. 2013; 143:484-491.
18. Guo J, Zhong R, Li WR, Liu YS, Bai ZJ, Yin J, *et al*. Interaction study on bovine serum albumin physically binding to silver nanoparticles: Evolution from discrete conjugates to protein coronas. Applied Surface Science, 2015; 359(5):82-88.
19. Rehman SU, Sarwar T, Ishqi HM, Husain MA, Hasan Z, Tabish, M. Deciphering the interactions between chlorambucil and calf thymus DNA: A multi-spectroscopic and molecular docking study. Archives of Biochemistry & Biophysics, 2015; 566(7):7-14.
20. Ross PD, Subramanian S. Thermodynamics of protein association reactions: forces contributing to stability. Biochemistry, 1981; 20(11):3096-3102.
21. Zhou H, Bi S, Wang Y, Zhao T. Characterization of the binding of paylean and DNA by fluorescence, UV spectroscopy and molecular docking techniques. Luminescence, 2016; 31(4):1013-1019.
22. Azimi O, Emami Z, Salari H, Chamani J. Probing the interaction of human serum albumin with norfloxacin in the presence of high-frequency electromagnetic fields: fluorescence spectroscopy and circular dichroism investigations. Molecules, 2011; 16(12):9792-9818.
23. Hu XX, Yu ZY, Liu RT. Spectroscopic investigations on the interactions between isopropanol and trypsin at molecular level. Spectrochemica Acta Part A Molecular & Biomolecular Spectroscopy, 2013; 108:50-54.
24. Cagnardi P, Villa R, Gallo M, Locatelli C, Carli S, Moroni P, *et al*. Cefoperazone sodium preparation behavior after intramammary administration in healthy and infected cows. Journal of Dairy Science. 2010; 93(9):4105-4110.
25. Liu YY, Zhang GW, Liao YJ, Wang YP. Binding characteristics of psoralen with trypsin: Insights from spectroscopic and molecular modeling studies.

Spectrochemica Acta Part A Molecular & Biomolecular Spectroscopy, 2015; 151:498-505.
26. Jana S, Dalapati S, Ghosh S, Guchhait N. Study of microheterogeneous environment of protein human serum albumin by an extrinsic fluorescent reporter: a spectroscopic study in combination with molecular docking and molecular dynamics simulation. Journal of Photochemistry & Photobiology B Biology. 2012; 112(231):48-58.